Regulations of mitoNEET by the key redox homeostasis molecule glutathione

Cécile Mons, Myriam Salameh, Thomas Botzanowski, Martin Clémancey, Pierre Dorlet, Cindy Vallières, Stéphane Erb, Laurence Vernis, Olivier Guittet, Michel Lepoivre, et al.

Journal of Inorganic Biochemistry 255 (2024) 112535

Contents lists available at ScienceDirect

Journal of Inorganic Biochemistry

journal homepage: www.elsevier.com/locate/jinorgbio

Regulations of mitoNEET by the key redox homeostasis molecule glutathione

Cécile Mons [a], Myriam Salameh [a], Thomas Botzanowski [b,c], Martin Clémancey [d], Pierre Dorlet [e,f], Cindy Vallières [a], Stéphane Erb [b,c], Laurence Vernis [a], Olivier Guittet [a], Michel Lepoivre [a], Meng-Er Huang [a], Sarah Cianferani [b,c], Jean-Marc Latour [d], Geneviève Blondin [d], Marie-Pierre Golinelli-Cohen [a,*]

[a] Université Paris-Saclay, Institut de Chimie des Substances Naturelles, CNRS UPR 2301, Gif-sur-Yvette cedex 91198, France
[b] Laboratoire de Spectrométrie de Masse BioOrganique, Université de Strasbourg, CNRS, IPHC UMR 7178, Strasbourg 67000, France
[c] Infrastructure Nationale de Protéomique ProFI – FR2048, Strasbourg 67000, France
[d] Université Grenoble Alpes, CEA, CNRS, Laboratoire de Chimie et Biologie des Métaux (LCBM), Grenoble 38000, France
[e] Université Paris-Saclay, CEA, CNRS, Institute for Integrative Biology of the Cell (I2BC), Gif-sur-Yvette cedex 91198, France
[f] CNRS, Aix Marseille Université, BIP, IMM, Marseille cedex 09 13402, France

ARTICLE INFO

Keywords:
NEET proteins
mitoNEET
CISD2
iron-sulfur protein
glutathione
thiyl radicals

ABSTRACT

Human mitoNEET (mNT) and CISD2 are two NEET proteins characterized by an atypical [2Fe-2S] cluster coordination involving three cysteines and one histidine. They act as redox switches with an active state linked to the oxidation of their cluster. In the present study, we show that reduced glutathione but also free thiol-containing molecules such as β-mercaptoethanol can induce a loss of the mNT cluster under aerobic conditions, while CISD2 cluster appears more resistant. This disassembly occurs through a radical-based mechanism as previously observed with the bacterial SoxR. Interestingly, adding cysteine prevents glutathione-induced cluster loss. At low pH, glutathione can bind mNT in the vicinity of the cluster. These results suggest a potential new regulation mechanism of mNT activity by glutathione, an essential actor of the intracellular redox state.

1. Introduction

MitoNEET (mNT), also known as CISD1, is a small homodimeric protein (13 kDa for each monomer) anchored to the outer mitochondrial membrane by its 32 N-terminal residues, and with the major part of the protein, including the C-terminal Fe-S binding domain, located in the cytosol. Each monomer binds one [2Fe-2S] cluster coordinated by three cysteines (C72, C74 and C83) and one histidine (H87) in a CDGSH domain like other members of the NEET protein family (the name of NEET proteins comes from the presence of the amino acid sequence Asn-Glu-Glu-Thr in these proteins), which also includes CISD2 and CISD3 in mammals. Although the biological activity of mNT is still debated, studies have shown its role in the regulation of iron and reactive oxygen species (ROS) homeostasis [1–3], in the regulation of lipid and glucose metabolism [2,4], in a repair pathway for damaged Fe-S proteins [3] and in cell proliferation in various cancers including breast cancer [5].

In vitro studies revealed that holo-mNT (the cluster-containing form of the protein) can transfer its Fe-S cluster to the apoform of diverse Fe-S proteins (the cluster-devoided form of the protein) [3,6–9]. Therefore, we and others proposed that mNT could act as a redox switch protein. In resting cells, mNT cluster would be reduced and would remain the protein in a dormant state. Oxidative insults would oxidize the cluster and mNT would thus switch to an active state capable of transferring its Fe-S cluster [7,10,11]. Our *in vitro* studies also revealed a very high sensitivity of the mNT cluster stability to pH variations, which led us to propose that mNT could also act as a pH sensor [6]. Human CISD2, another member of the NEET family, was shown to be anchored to the endoplasmic reticulum (ER) membranes at mitochondrial contact sites with its Fe-S cluster in the cytosol like mNT. Nevertheless, despite the very high structural homology between the cytosolic domains of mNT and CISD2, we have previously shown that their Fe-S clusters exhibit very different biochemical properties. CISD2 cluster is more stable in the presence of oxygen than that of mNT and is also more difficult to transfer. Moreover, its stability and transferability are only slightly

* Corresponding author at: Institut de Chimie des Substances Naturelles, UPR 2301-CNRS, 1 avenue de la Terrasse, Gif-sur-Yvette 91190, France.
E-mail address: marie-pierre.golinelli@cnrs.fr (M.-P. Golinelli-Cohen).

https://doi.org/10.1016/j.jinorgbio.2024.112535
Received 16 November 2023; Received in revised form 29 February 2024; Accepted 19 March 2024
Available online 20 March 2024

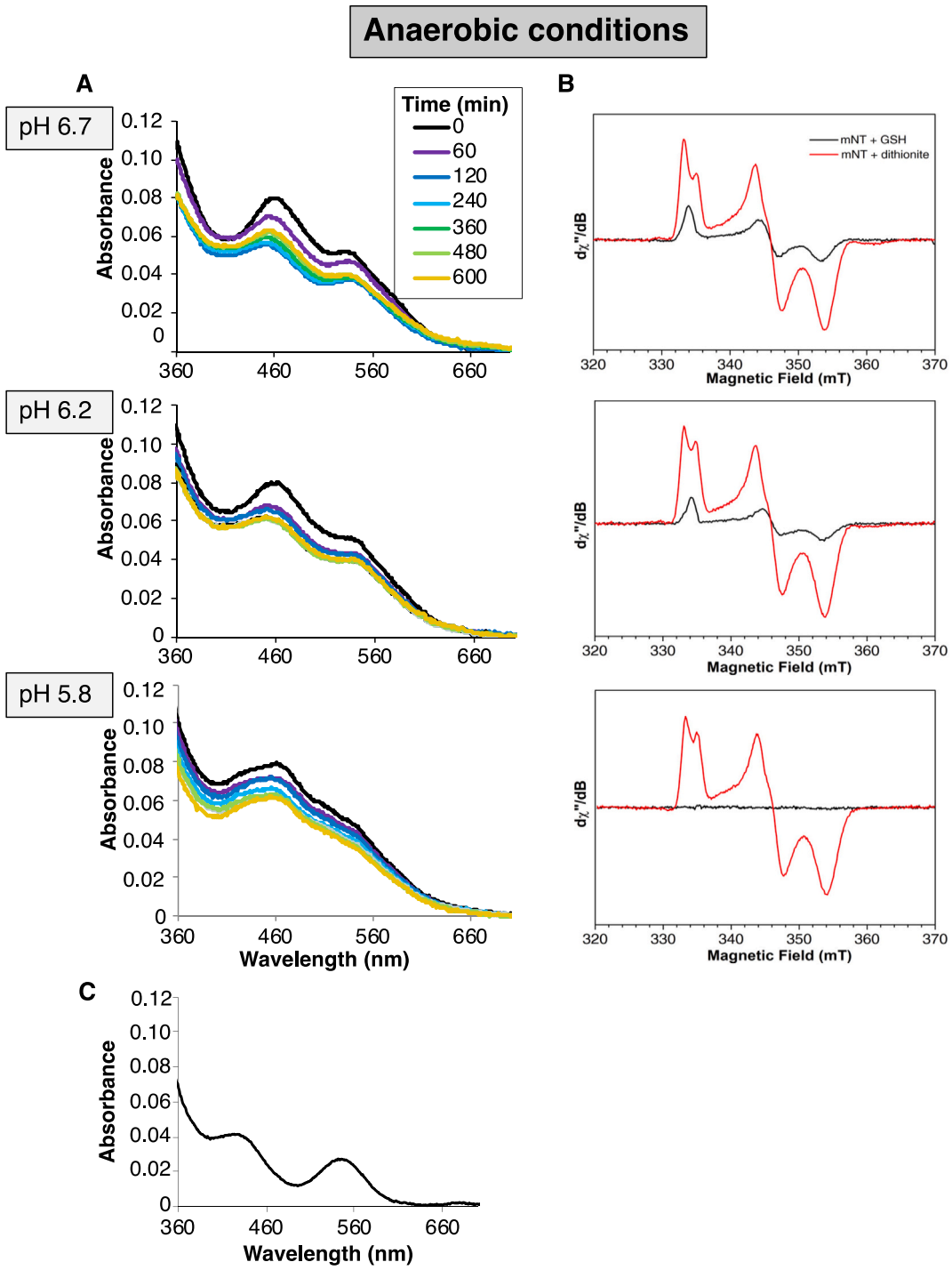

Fig. 1. GSH induces a partial reduction of oxidized mNT's cluster in the absence of oxygen. mNT cluster loss reactions (20 μM of protein) were performed at 15 °C under anaerobic conditions in the presence of 10 mM GSH in 100 mM NaCl 100 mM Bis-Tris at pH 6.7, 6.2 and 5.8. **(A)** The reaction was followed by UV–visible absorption spectroscopy. Experiments were performed in triplicate. One representative serie is presented. **(B)** The EPR spectra were recorded on the samples after 2 h reaction (panel B, black curves). Controls for each corresponding pH values were performed by addition of 2 mM dithionite (red curves). The EPR spectrum of the oxidized mNT sample did not show any Fe-S cluster signal and was used as baseline and subtracted from all spectra. **(C)** UV–visible absorption spectrum of 20 μM mNT reduced by 2 mM DTT. (For interpretation of the references to colour in this figure legend, the reader is referred to the web version of this article.)

affected by pH variations in contrast to that of mNT [12].

Glutathione, the γ-L-glutamyl-L-cysteinyl-glycine tripeptide, is the most abundant water-soluble non-protein thiol in the cell (1 to 10 mM in eukaryotic cells) and is present in all tissues. It has a large number of essential functions in metabolism, catalysis and transport. It also plays a major role in maintaining cellular redox balance and in detoxification [13]. The molecule exists in two redox states: the reduced form (GSH) and the oxidized form (GSSG). Glutathione is mostly present in its reduced form (>98%) in resting cells [14]. It regulates ROS at low levels, is essential for redox cell signaling involved in many life processes, and limits excessive oxidative stress (high concentration of ROS) that leads to cell damages. Dysregulation of GSH homeostasis is associated with

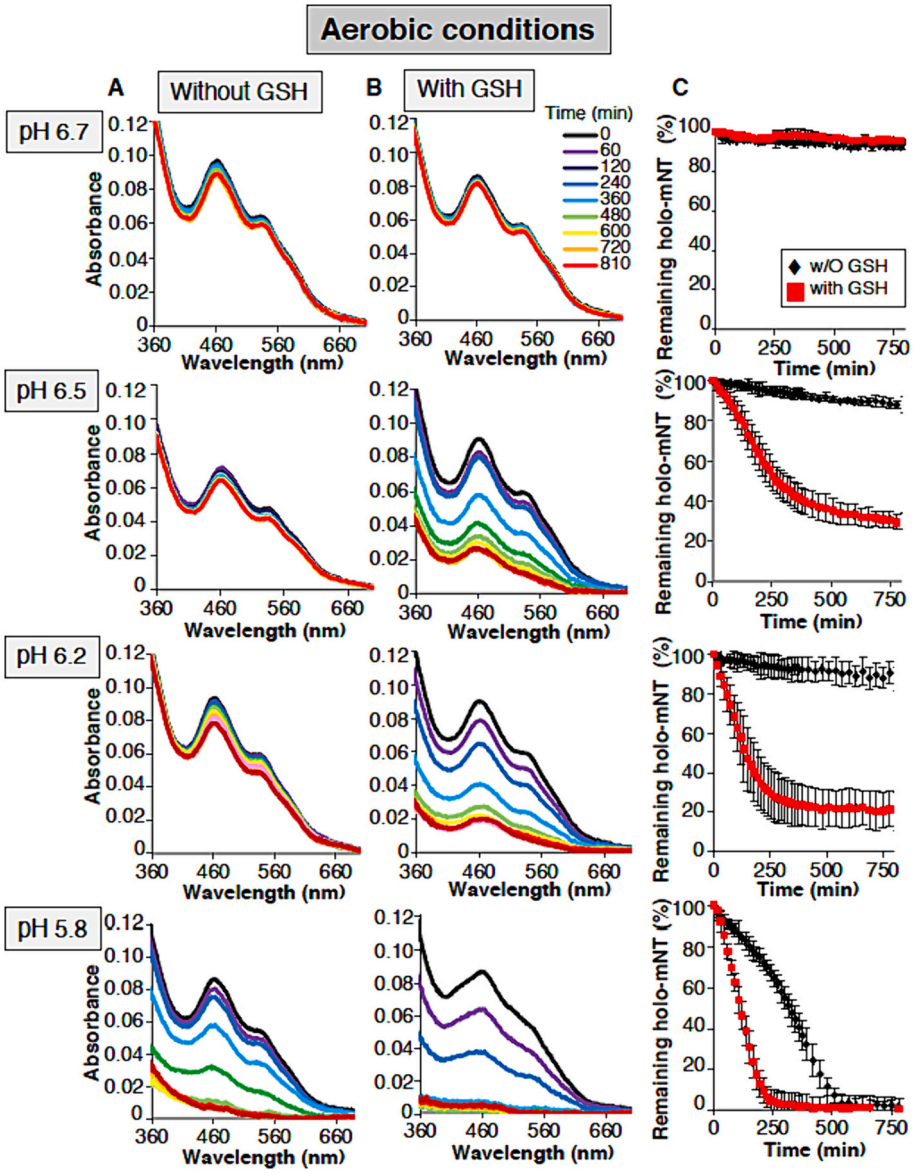

Fig. 2. GSH induces a loss of oxidized mNT Fe-S cluster in the presence of oxygen. mNT cluster loss reactions (20 μM of protein) were performed at 15 °C under aerobic conditions in the absence **(A)** or the presence **(B)** of 10 mM GSH in 100 mM Bis-Tris (pH 6.7/6.5/6.2/5.8) 100 mM NaCl. The percentage of remaining holo-mNT determined from the absorbance at 460 nm was then plotted over time **(C)**. Curves from reactions performed in the absence of GSH are plotted with black diamonds and those performed in the presence of 10 mM GSH are represented with red squares. Experiments were performed in triplicate. The curves are the mean of the data and the error bars are the associated standard deviations. (For interpretation of the references to colour in this figure legend, the reader is referred to the web version of this article.)

many human diseases such as cardiovascular diseases [15], chronic obstructive pulmonary disease, but also in cancer and severe acute respiratory syndrome coronavirus 2 disease (COVID-19) [16]. Therapies increasing GSH levels are being considered to treat or prevent these diseases [17]. Glutathione is also intimately linked to iron metabolism, and to Fe-S cluster biogenesis [18], export and trafficking [19,20]. It has been shown that GSH could stabilize the Fe-S cluster of some proteins. For example, the mitochondrial glutaredoxins GLRX5, a key component of the mitochondrial Fe-S cluster (ISC) machinery, exhibits a GSH-dependent binding of its Fe-S cluster [21]. Moreover, the export of a sulfur-containing component out of the mitochondria, essential for the maturation of cytosolic Fe-S-containing proteins, is dependent on GSH [18,22,23]. GSH could also extrude the Fe-S cluster of some proteins and form a stable species composed of GSH, iron and sulfur ($[2Fe\text{-}2S](GS)_4$) [24,25]). It may also improve cluster trafficking between proteins at least *in vitro* [26]. In *Mycobacterium tuberculosis* WhiB proteins, GSH protects the Fe-S cluster from oxidative degradation [27]. However, a loss of the cluster induced by GSH was also observed in the case of SoxR [28], a bacterial transcription factor, which, like mNT, is regulated by the redox state of its Fe-S cluster [10]. In the case of mNT, GSH, like several other thiols (cysteine (Cys), *N*-acetyl-cysteine, or dithiothreitol), has previously been shown to reduce, at least partially, the Fe-S cluster of mNT under anaerobic conditions *in vitro* [29]. However, compared to the other tested reductants, GSH has the lowest capacity to reduce the cluster although its redox potential (−0.240 V) is lower than that of L-Cys (−0.220 V) at pH 7 [30].

Considering that mNT cluster transfer is regulated by the redox state of its cluster and that the protein seems to be involved in cellular responses to stress, we wondered about a possible regulation of mNT by glutathione beyond the simple cluster reduction already observed by others [29]. We therefore conducted a detailed study of the effect of GSH, but also of other molecules with a thiol function, on the Fe-S

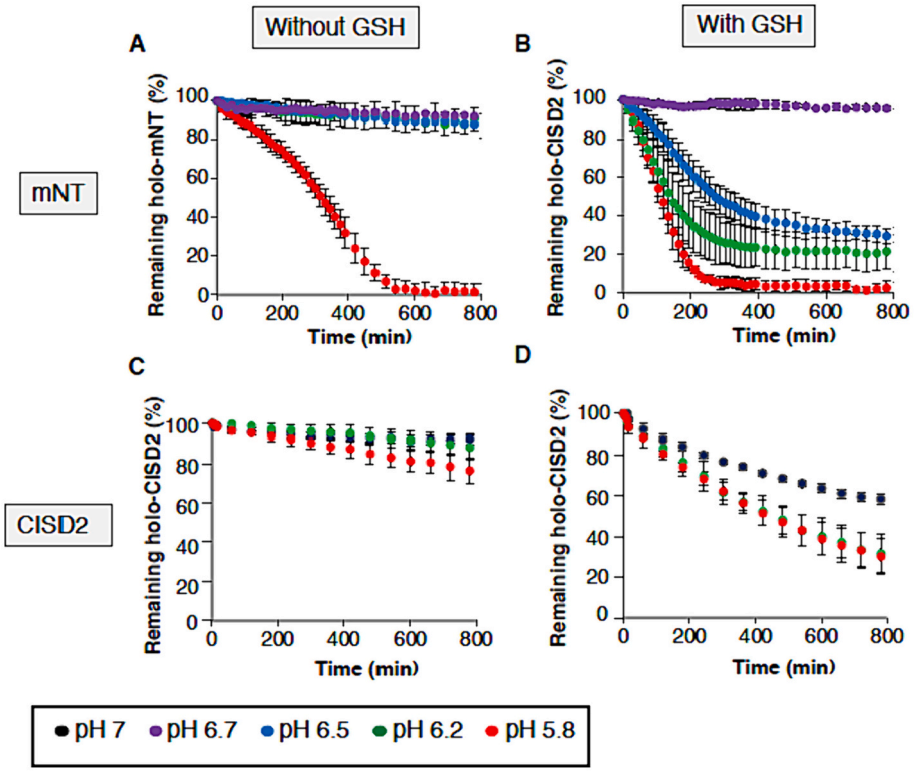

Fig. 3. CISD2 is less sensitive to GSH-induced Fe-S cluster loss than mNT. mNT **(A and B)** and CISD2 **(C and D)** cluster loss reactions (20 μM of protein) were performed at 15 °C under aerobic conditions in the absence **(A and C)** or the presence **(B and D)** of 10 mM GSH in 100 mM Bis-Tris/Tris 100 mM NaCl buffer at pH 7 (black), 6.7 (violet), 6.5 (blue), 6.2 (green) and 5.8 (red). The percentage of remaining holo-mNT/CISD2 determined from the absorbance at 460 nm was then plotted over time. Experiments were performed in triplicate. The curves are the mean of the data and the error bars are the associated standard deviations. (For interpretation of the references to colour in this figure legend, the reader is referred to the web version of this article.)

cluster of mNT. We found that GSH can induce Fe-S cluster loss through a radical mechanism and also bind to mNT in the vicinity of its cluster. In contrast, CISD2 Fe-S cluster appears to be only weakly sensitive to GSH compared to mNT Fe-S cluster. Glutathione, an essential molecule required for redox homeostasis in eukaryotes, may thus possibly regulate mNT activities in cells. In this manuscript, we will refer to as "cluster loss" the fact that a protein with an Fe-S cluster (holoform) loses its Fe-S cluster (conversion of the protein to an apoform) without presuming the exact fate of the ions originally forming this Fe-S cluster.

2. Materials and methods

2.1. Chemicals

Reduced and oxidized glutathione, cysteine, cystine, β-mercaptoethanol, 5,5-dimethyl-1-pyrroline N-oxide (DMPO), *N*-acetyl-L-cysteine, L-cysteine methyl ester, D,L-penicillamine were purchased from Merck. Because glutathione is highly acidic and mNT is sensitive to pH-variation, 250 mM solutions were prepared in 500 mM BisTris/Tris-HCl at the pH of the reaction (typically between pH 5.8 and 7.0). The pH was checked and adjusted when necessary by addition of 5 M NaOH solution. Solutions were aliquoted and kept at −20 °C. We checked the reduced state of the reduced glutathione solution by colorimetric assay [31] and found that the solution oxidized at around 2% per hour under the reaction conditions.

2.2. Purification of human mNT and CISD2

Holo-forms of human $mNT_{44–108}$ missing the 43 N-terminal amino acids (WT and H87C forms) were expressed in bacteria and purified as previously described [32] then stored at −80 °C. For Mössbauer analysis, expression of $mNT_{33–108}$ missing the 32 N-terminal amino acids was performed using the pET28a-$mNT_{33–108}$ construct in M9 minimal medium supplemented with ^{57}Fe-enriched ferric chloride. The N-terminal His tag of purified $mNT_{33–108}$ was removed efficiently using thrombin [3]. Holo-CISD2 was purified as previously described [12]. Protein purity was assessed to be >99% using SDS-PAGE. For both proteins, the optical A_{280nm}/ A_{458nm} ratio was around 2.4. Protein concentrations were measured using Bradford assay with bovine serum albumin (BSA) as standard. Using an extinction coefficient at 456 nm of 5000 cm^{-1} M^{-1} [1], we checked that the purified protein was at least 90% in the holo-form.

2.3. In vitro mNT cluster loss reaction

Reaction buffers were all composed of 100 mM NaCl and 100 mM Bis-Tris (pH from 5.8 to 7.0). UV–visible absorption spectra were recorded at 15 °C between either 240 to 900 nm or 350 to 900 nm with a Cary 100 (Agilent) spectrophotometer equipped with a temperature control apparatus. For spectra taken under anaerobic conditions, the cuvette was prepared in a glove box (Jacomex) and closed with a septum. The absorption spectra of the reaction mixture were recorded over time and corrected for baseline variations at 900 nm. The extent of the loss of oxidized mNT cluster was determined using the absorbance at 460 nm (A_{460}). As previously described [32], reaction progress at time t was estimated as $(A_{460}\ (t) - A_{460,initial})/(A_{460,final} - A_{460,initial})$. $A_{460,final}$ is the value of A_{460} at the time necessary for reaction completion. For reactions performed in presence of DMPO, the reaction mixtures were analyzed on a native gel, which allows the separation of the apo- and holo-forms of mNT [32]. After Blue Silver staining of the gel [33], the intensity of the holo-form band was quantified using Odyssey Infrared Imaging System (LI-COR). $T_{1/2}$ is the time required for half of the cluster

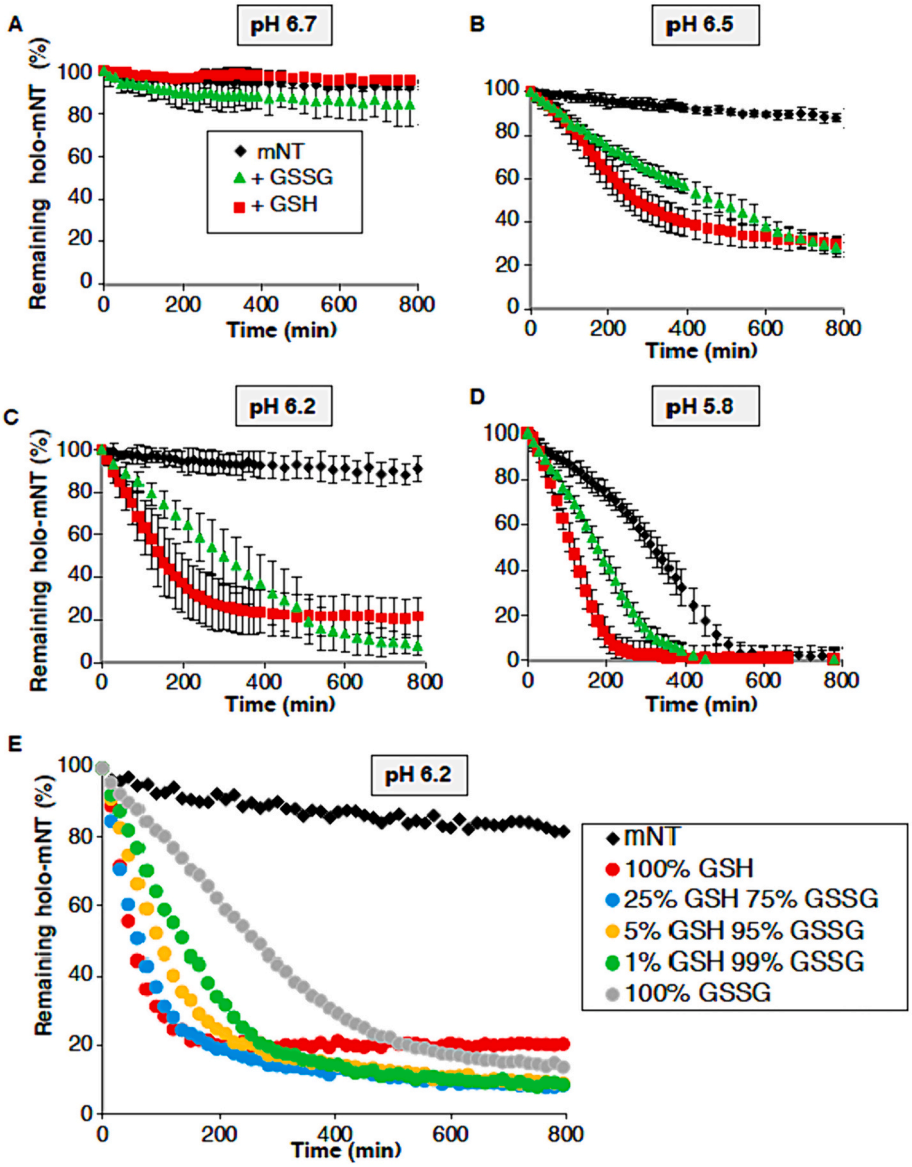

Fig. 4. Effects on mNT Fe-S cluster is dependent on the redox state of glutathione. mNT cluster loss reactions (20 μM of protein) were performed at 15 °C under aerobic conditions. **(A-D)** Reactions were performed in the absence (black) or the presence of either 10 mM GSH (red) or GSSG (green) in 100 mM NaCl 100 mM Bis-Tris pH 6.7 **(A)**, pH 6.5 **(B)**, pH 6.2 **(C)** and pH 5.8 **(D)**. The percentage of remaining holo-mNT determined from the absorbance at 460 nm was then plotted over time. Experiments were performed in triplicate. The curves are the mean of the data and the error bars are the associated standard deviations. **(E)** Reactions were performed in 100 mM Bis-Tris pH 6.2100 mM NaCl under aerobic conditions in the absence of glutathione (black) or in the presence of 10 mM glutathione in various GSH/GSSG ratio. The percentage of remaining holo-mNT determined from the absorbance at 460 nm was then plotted over time. Experiments were performed in triplicate. One representative series of experiments is represented for the clarity of the figure. (For interpretation of the references to colour in this figure legend, the reader is referred to the web version of this article.)

to be lost.

2.4. Mass spectrometry analysis

Ammonium acetate ($AcONH_4$, catalog no. A1542) and high-grade acetonitrile (catalog no. 34851) were purchased from Sigma-Aldrich. Aqueous solutions were prepared using an ultrapure water system (Sartorius, Göttingen, Germany). Native mass spectrometry measurements were performed in positive ion mode on an electrospray time-of-flight mass spectrometer (LCT, Waters, Manchester, U.K., upgraded by MS Vision) equipped with an automated chip-based nanoESI source (Triversa Nanomate, Advion). The instrument was calibrated using a 2 μM horse heart myoglobin solution. Analyses under native conditions were performed after careful optimization of instrumental settings to avoid dissociation of noncovalent interactions and to obtain sensitive detection of protein/Fe-S clusters. Cone voltage (Vc) and backing pressure (bP) were fixed to 20 V and 6 mbar, respectively. Native MS experiments were performed in triplicate under identical conditions at 0, 0.5, 1 h at room temperature. Acquisitions were performed in the mass range of m/z 20–5000 with a 4 s scan time. Both positively and negatively charged species were searched. Data analysis was performed with MassLynx version 4.0 (Waters, Manchester, U.K.).

2.5. Mössbauer spectroscopy

Mössbauer spectra of purified ^{57}Fe-labeled $mNT_{33–108}$ were recorded at 4.8 K on a low-field Mössbauer spectrometer equipped with a Janis CCR 5 K cryostat. The spectrometer was operated in a constant

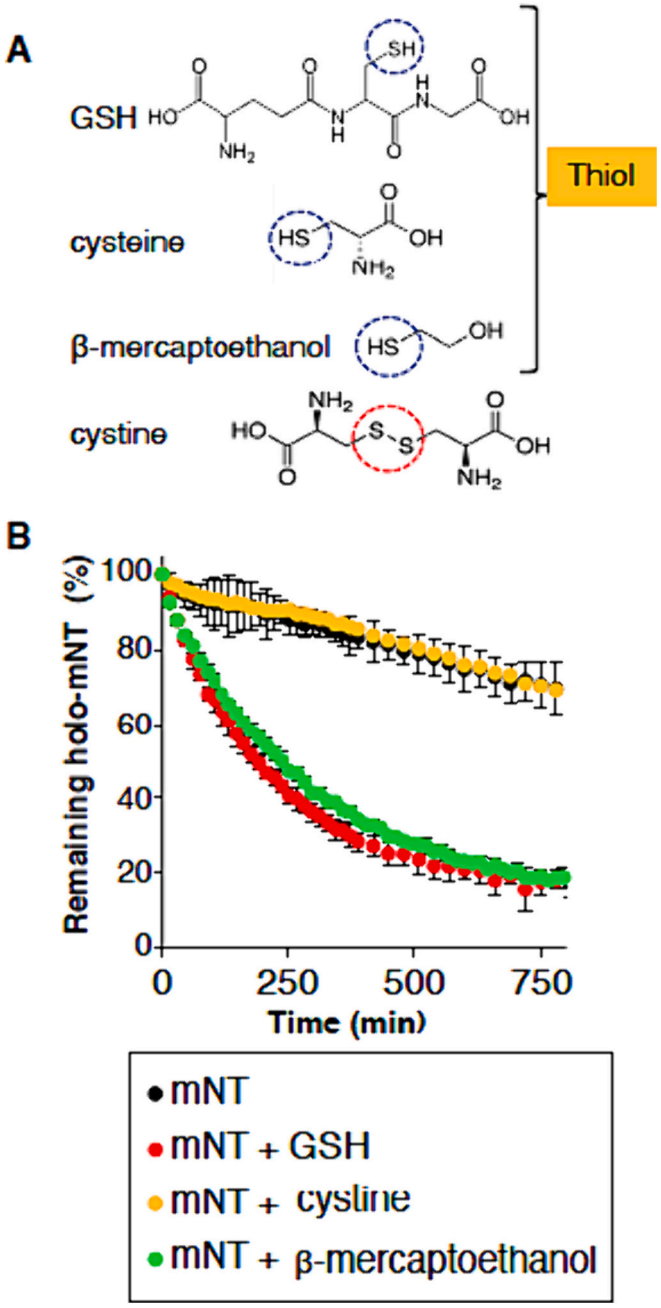

Fig. 5. Thiol-containing molecules induces mNT Fe-S cluster loss. (A) Structures of the studied molecules. Thiol groups are highlighted by a blue dotted circle and disulfide bonds by a red dotted circle. **(B)** mNT cluster loss reactions (20 μM of protein) were performed at 15 °C in 100 mM Bis-Tris pH 6.5100 mM under aerobic conditions in the absence of any additive (black) or in the presence of 1 mM of GSH (red), cystine (orange) or β-mercaptoethanol (green). The percentage of remaining holo-mNT determined from the absorbance at 460 nm was then plotted over time. Experiments were performed in triplicate. The curves are the mean of the data and the error bars are the associated standard deviations. (For interpretation of the references to colour in this figure legend, the reader is referred to the web version of this article.)

acceleration mode in transmission geometry. The isomer shifts were referenced against a metallic iron foil at room temperature. Data were analyzed with the WMOSS program Mössbauer Spectral Analysis Software (www.wmoss.org, 2012–2013, Web Research, Edina).

Table 1
Effect of thiols on mNT Fe-S cluster.

Thiol effects	Thiols
Disruptive	glutathione
	N-acetyl-L-cysteine
	L-cysteine methyl ester
	β-mercaptoethanol
	D,L penicillamine
Protective	cysteine
No effect	cystine

2.6. EPR spectroscopy

EPR spectra were measured in continuous mode using a Bruker Elexsys E500 spectrometer equipped with a high-sensitivity cavity and a helium continuous flow cryostat (Oxford Instrument) connected to a temperature control system. The frequency of the spectrometer was 9.37 GHz, the temperature 30 K and the microwave power 1 mW. The samples (180 μL) were prepared in a glove box and then frozen under anaerobic conditions. They all contained 20 μM of mNT to which 2 mM dithionite (30-min incubation), or 10 mM GSH (2-h incubation) were added and incubated before freezing. The solutions of dithionite and GSH were buffered due to the high sensitivity of mNT cluster to small pH changes [6].

3. Results

3.1. GSH induces a partial reduction of mNT Fe-S cluster in the absence of oxygen

We showed previously that oxidized mNT is highly stable in the absence of oxygen (anaerobic conditions) and very little cluster loss was observed after 10 h even at low pH (pH 5.8) [6]. In the present study, we first determined at the effect of GSH on oxidized mNT cluster under anaerobic conditions (Fig. 1).

By UV–visible absorption, we observed a slight decrease of the absorbance in the visible part but also a deformation of the spectrum over time (Fig. 1 panel A). The spectral deformation increases as the pH was lowered, and is well distinguished at pH 5.8. EPR studies (Fig. 1 panel B) revealed that addition of GSH at pH 6.7 only partially reduced the cluster as shown by others [29]. By comparison to reduction obtained by addition of dithionite, the amount of reduced cluster following the addition of GSH was <25% after 2 h at pH 6.7 and was even more limited when the pH decreased with 15% at pH 6.2 and absent at pH 5.8 (panel B). In addition, we observed that the line shape of the EPR signal for the partially GSH-reduced cluster differs from that of the fully dithionite-reduced cluster as previously observed [34]. The splitting around 334–336 mT observed for the fully reduced sample is due to the interaction between the two reduced clusters [34]. In the absence of oxygen, addition of GSH to oxidized mNT did not significantly destabilize the cluster. However, it led to modification of the UV–visible absorption spectra that cannot be only explained by the cluster reduction (Fig. 1 panel C).

3.2. GSH can induce a rapid loss of oxidized mNT cluster in the presence of oxygen

Under aerobic conditions at 15 °C in the absence of GSH, mNT cluster was rather stable down to pH 6.2 and its lability increased as the buffer became more acidic (Fig. 2 panel A) as expected [6].

Then we examined at the effect of addition of GSH on mNT's cluster under aerobic conditions. It can be noticed that a 2% oxidation per hour of the reduced glutathione was observed during the experiments. Thus all the specified concentrations of GSH but also of the other thiol-containing molecules used in this study referred to the initial concentrations of the molecules. GSH had no significant effect on the stability of

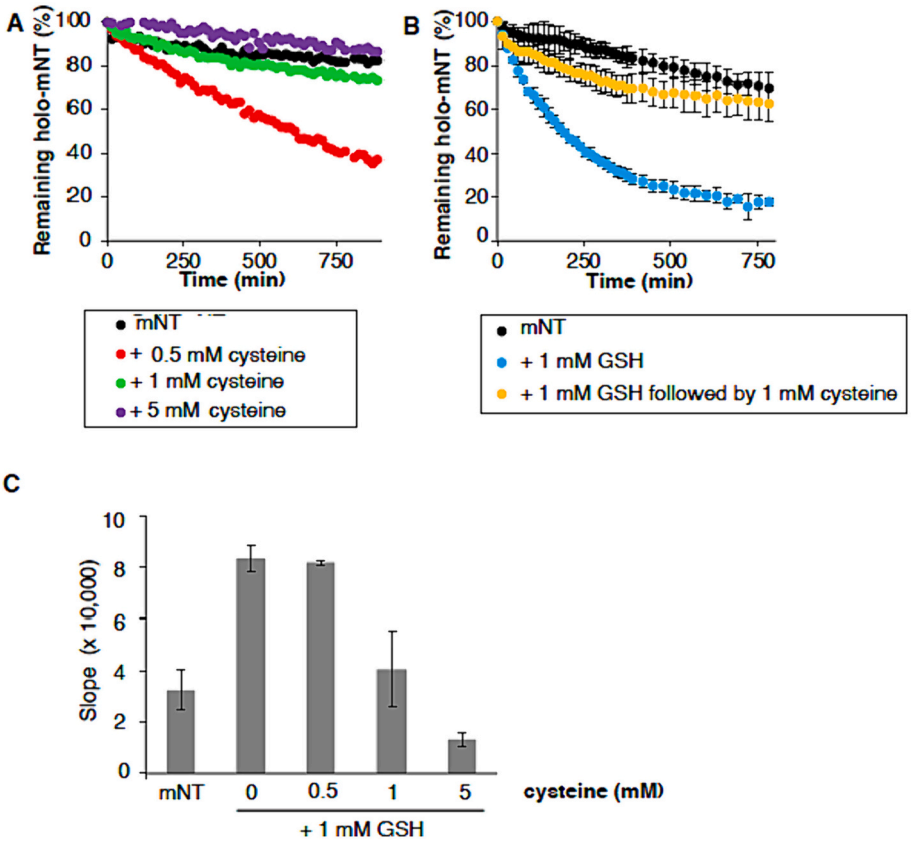

Fig. 6. Cysteine can protect mNT cluster from GSH. mNT cluster loss reactions (20 μM of protein) were performed at 15 °C in 100 mM Bis-Tris pH 6.5100 mM NaCl under aerobic conditions. **(A)** Reactions were performed without any additive (black) or in the presence of 0.5 mM (red), 1 mM (green) or 5 mM (purple) cysteine. The percentage of remaining holo-mNT determined from the absorbance at 460 nm was then plotted over time. Experiments were performed in triplicate. One representative series of experiments is shown. **(B)** Reactions were performed without any additive (black), or in the presence of 1 mM GSH (yellow and blue). We added 1 mM L-cysteine 30 min after GSH addition (yellow). The percentage of remaining holo-mNT determined from the absorbance at 460 nm was then plotted over time. Experiments were performed in triplicate. The curves are the mean of the data and the error bars are the associated standard deviations. **(C)** Reactions were performed either without addition of any molecule ("mNT" lane) or in the presence of 1 mM GSH. L-cysteine was added in various concentrations (0, 0.5, 1 or 5 mM) 30 min after GSH addition. Cluster loss reactions were followed by UV–visible absorption spectroscopy. The absorbance at 460 nm is plotted over time. The slope of the curve ("slope") at 35 min is plotted as a function of the reaction conditions. Experiments were performed in triplicate. The histogram is the mean of the data and the error bars are the associated standard deviations. (For interpretation of the references to colour in this figure legend, the reader is referred to the web version of this article.)

oxidized mNT cluster at pH 6.7 (Fig. 2 top panel B). However, at lower pH levels, the addition of GSH induced a loss of the cluster, which increased as the buffer became more acidic (Fig. 2 panel B and C). While GSH had no effect at pH 6.7, the $T_{1/2}$ was 300 min, 130 min and 110 min at pH 6.5, 6.2 and 5.8 respectively. We performed similar experiments with oxidized CISD2 (Fig. 3) without (panel C) and with GSH (panel D).

GSH induced a more limited loss of CISD2 cluster compared to mNT's one (Fig. 3 panels A and B). This was accompanied by a more limited pH dependency for CISD2 with a $T_{1/2}$ at pH 5.8 of 420 min compared to 110 min for mNT at the same pH. Thus, the Fe-S cluster of mNT under aerobic conditions is more sensitive to GSH than that of CISD2. For the rest of the study we decided to focus on mNT to better understand its sensitivity to GSH.

3.3. The redox state of glutathione affects the cluster loss

We then questioned the effect of the oxidation state of glutathione on the stability of mNT cluster (Fig. 4).

At pH 6.7, addition of GSSG, the oxidized form of glutathione, did not significantly destabilize the cluster (Fig. 4 panel A) as with GSH. At lower pH, it induced a more limited cluster loss than GSH (Fig. 4 panels B-D). Then, we added a fixed concentration of glutathione (GSH + GSSG, 10 mM) with a variable ratio GSH/GSSG (Fig. 4 panel E). The experiment was performed at pH 6.2, a condition in which the addition of GSH led to a significant but not too fast cluster loss. Even with only 25% GSH, the loss of cluster was similar to that obtained with 100% GSH. The addition of only 1% GSH significantly accelerated the loss of the cluster compared to GSSG alone. Therefore, even at low GSH/GSSG ratios, the effect of GSH predominated over that of GSSG. From this experiment, we can estimate that the 100 μM GSH induced a loss of the Fe-S cluster whose rate is 50% of the maximum rate of loss of Fe-S cluster obtained with higher GSH concentrations. Experiments performed with variable concentrations of GSH (in the absence of GSSG) led to the same result (data not shown).

3.4. Thiol-containing molecules destabilize oxidized mNT cluster

In order to determine whether this effect is specific to glutathione or not, we tested the impact of different sulfur-containing molecules. As GSH, cysteine (Cys) and β-mercaptoethanol have a thiol function while cystine does not (Fig. 5 panel A).

Typically, the molecules containing a free thiol function were able to destabilize mNT cluster at 1 mM (Fig. 5 panel B and Table 1).

As GSH, Cys has a free thiol function but its effect on the cluster loss was different. At a concentration of 0.5 mM, Cys destabilized the cluster (Fig. 6 panel A) as expected. A cysteine concentration as low as 50 μM

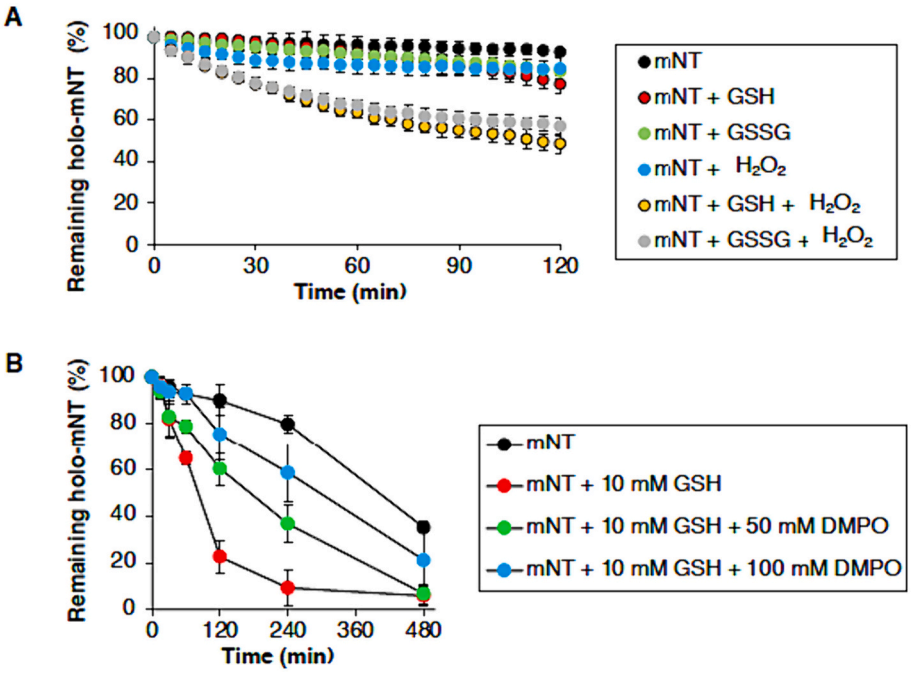

Fig. 7. Formation of thiyl radicals induces mNT cluster loss. mNT cluster loss reactions (20 μM of protein) were performed at 15 °C in 100 mM Bis-Tris pH 6.2100 mM NaCl under aerobic conditions. **(A)** Reactions were performed in the absence of any additive (black) or in the presence of 1 mM of GSH (red), GSSG (green), H_2O_2 (blue), GSH and H_2O_2 (orange) or GSSG and H_2O_2 (grey). The percentage of remaining holo-mNT determined from the absorbance at 460 nm was then plotted over time. Experiments were performed in triplicate. The curves are the mean of the data and the error bars are the associated standard deviations. **(B)** Reactions were performed in the absence of GSH (black), or in the presence of either 10 mM GSH (red) or 10 mM GSH with 50 mM (green) or 100 mM DMPO (blue). Reactions were analyzed on native gels and the amount of remaining holo-mNT was quantified. The percentage of remaining holo-mNT was then plotted over time. Experiments were performed in triplicate. The curves are the mean of the data and the error bars are the associated standard deviations. (For interpretation of the references to colour in this figure legend, the reader is referred to the web version of this article.)

led to cluster loss similarly to what was observed with 500 μM cysteine (data not shown). However, higher concentrations of Cys (1 to 5 mM) had no effect on the cluster. We next questioned if Cys at high concentration could protect mNT from GSH-induced cluster loss. After incubating oxidized mNT with 1 mM GSH for 30 min, 1 mM Cys was added (Fig. 6 panel B), the rate of Fe-S cluster loss was slowed down (yellow curve) compared to the experiment performed in the presence of GSH only (blue curve). Note that if 1 mM GSH was added instead of 1 mM Cys, no such protective effect was observed.

Other Cys concentrations were also tested (Fig. 6 panel C) in the presence of 1 mM GSH. For concentrations higher than 0.5 mM, Cys slowed down the cluster loss induced by GSH and the protective effect increased with the concentration of Cys (Fig. 6 panel C).

3.5. Radical species derived from GSH are responsible for cluster loss

For the rest of the study, we focused on glutathione. Glutathione, in its oxidized and reduced forms, is known to be a source of radicals including thiyl radicals formed by the reaction of the thiol group with ROS [35,36]. As described above, we observed the importance of oxygen in the cluster loss of mNT by GSH (compare results under anaerobic conditions in Fig. 1 and aerobic conditions in Fig. 2) which leads to question the role of radicals derived from GSH in the loss of the Fe-S cluster. First, we sought to increase the production of radicals by reaction of GSH with ROS. For this purpose, we simultaneously added GSH or GSSG with H_2O_2. The experiment was performed under specific conditions (time, pH, glutathione and H_2O_2 concentrations) so that the addition of glutathione (1 mM) (Fig. 7 panel A, red and green curves) or H_2O_2 (1 mM) (blue curve) alone induced only a very limited loss of the cluster.

On the contrary, we found that the simultaneous addition of glutathione (either GSH or GSSG) and H_2O_2 (orange and grey curves) significantly increased the rate of the cluster loss. Then, the concentration of potential radical species using DMPO was decreased, which reacts with radicals and form a stable adduct. Because DMPO strongly absorbs at visible wavelengths, we followed the reactions on native gels [32]. The loss of the Fe-S cluster in NEET proteins leads to changes of protein structure as demonstrated previously for mitoNEET [3] and CISD2 [12]. The apo and holo forms indeed displayed different migrations pattern on native PAGE gels [32]. In the presence of DMPO, the loss of Fe-S cluster induced by GSH was slowed down (Fig. 7 panel B). This protective effect increased with the concentration of DMPO.

3.6. Glutathione binds to mNT close to the cluster

The fine analysis of the UV–visible absorption spectra showed that the addition of GSH at pH 5.8 induced a significant distortion of the UV–visible absorption spectrum of oxidized mNT in both anaerobic (Fig. 1 panel A) and aerobic conditions (Fig. 2 panel B). Two hypotheses can be formulated to explain this result. First, GSH could extract the Fe-S cluster from mNT and form a stable species composed of GSH, iron and sulfur, namely ([2Fe-2S](GS)$_4$) [24,37], as previously proposed for human ISCU, *S. cerevisiae* GRX3 or *S. pombe* Isa1 [38]. The UV–visible absorption spectrum would then be a combination of holo-mNT and ([2Fe-2S](GS)$_4$) absorptions [24,39,40]. The second hypothesis is that GSH binds to or is close to the Fe-S cluster of mNT and affects the Fe-S charge transfer. Indeed, the visible part of the UV–visible absorption spectrum of an Fe-S protein is related not only to the nature but also to the environment of the cluster. Analysis of the UV–visible absorption spectra showed that the addition of GSH induced the appearance of a new absorption band at higher energy, which led to an asymmetry of the absorption peak around 460 nm, characteristic of the oxidized mNT's [2Fe-2S] cluster (Fig. 8 panel A, compare black and red curves).

Moreover, this spectral deformation is observable (Fig. 8 panel C)

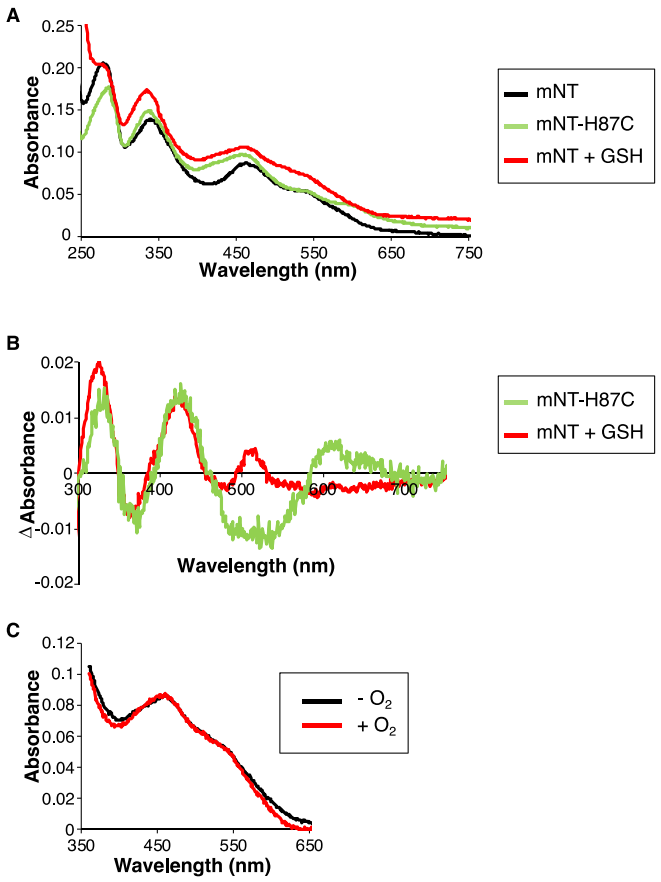

Fig. 8. Reduced glutathione induces a modification of the UV–visible absorption of oxidized mNT. All the experiments were performed in 100 mM Bis-Tris pH 5.8100 mM NaCl with 20 μM mNT. **(A)** UV–visible absorption spectra of oxidized mNT without (black) or with 10 mM GSH (red) and of oxidized H87C mutated form of mNT (green). The baseline of the H87C mutated form was incremented by 0.015 and that of WT mNT in the presence of GSH by 0.030 for a better readability of the figure. (B) Difference spectra from panel A. "mNT-H87C" is the difference between the spectrum of mNT-H87C and mNT. "mNT + GSH" is the difference spectrum between the spectrum of mNT + GSH and mNT. **(C)** Comparison of the UV–visible absorption spectra of oxidized mNT in presence of 10 mM GSH under aerobic (red) and anaerobic (black) conditions at 15 °C. (For interpretation of the references to colour in this figure legend, the reader is referred to the web version of this article.)

under both anaerobic (black curve) and aerobic (red curve) conditions thus, not associated with the presence of oxygen. We analyzed the spectrum of the H87C mutated form, with the histidine 87 ligand of the cluster replaced by a cysteine. In this mutated form the cluster was no coordinated by 3 cysteines and 1 histidine anymore but by 4 cysteines [41]. Very interestingly, the spectrum of the H87C was similar to that of the wild-type (WT) form in presence of GSH (Fig. 8 panel A). Below 550 nm, both spectra were very similar (Fig. 8 panel B).

We then analyzed the GSH reaction product by native mass spectrometry on WT mNT. As native MS (nMS) is not compatible with the presence of non-volatile NaCl salts in the samples, the study was performed in an aqueous buffer composed of 50 mM ammonium acetate at pH 5.8. In these conditions, the spectral distortion of the UV–visible absorption spectrum was observed in a similar manner as in the BisTris buffer (data not shown). In the absence of GSH, the main species detected in nMS corresponded to monomeric and dimeric holo-mNT, while a minor apo-mNT monomeric form was also observed (Fig. 9 upper parts of panels A and B, supplementary Fig. 1) in agreement with our previously reported data [6].

In the presence of GSH (30 min incubation), the nMS spectra were much more complex and several monomeric and dimeric species were detected (Fig. 9 middle panels) but the $[2Fe\text{-}2S](GS)_4^{2-}$ was never observed even if negatively charged species were also searched. As for the monomers (Fig. 9 panel A), three main species were observed: apo-mNT, apo-mNT bound to one GSH and holo-mNT (Fig. 9 panel A, middle panel). Only very minor monomeric signals corresponding to the binding of 2 GSH on apo-mNT and 1 GSH on holo-mNT were observed. These observations suggest that after 30 min of GSH incubation (Fig. 9,lower panel A), GSH binding led to a rapid ejection of two iron atoms and one sulfur atom, the second sulfur atom from the Fe-S cluster being partially retained (roughly 50% of the apo-protein is bound to GSH that retained one sulfur atom). This sulfur was not lost even after 60 min incubation while GSH remained attached to apo-mNT. On the dimeric side (Fig. 9 panel B), the cluster loss was less obvious and main species correspond to $(holo\text{-}mNT)_2$. Only very minor nMS signals corresponding to $(holo\text{-}mNT)_2$ bearing one or two GSH molecules were detected, their intensities did not increase after 60 min incubation. Altogether nMS results clearly demonstrate a loss of the Fe-S cluster of the holo-mNT monomeric form in presence of GSH, leading to ejection of two iron atoms and one sulfur atom, along with partial retention of the second sulfur atom from the Fe-S cluster. This retention of a sulfur atom is a hallmark of GSH binding to mNT in agreement with our previously published results highlighting that in the absence of GSH, all the atoms of the Fe-S cluster of mNT are lost simultaneously [6].

We then characterized the reaction products by Mössbauer spectroscopy. First, the spectrum of mNT alone was measured (Fig. 10 panel A).

The parameters (isomeric shift δ and quadrupolar coupling ΔE_Q) were similar to those we obtained at pH 8 [3]. The spectrum measured in presence of GSH (Fig. 10 panel B), in addition to the starting oxidized mNT, revealed the presence of additional species. The absorption observed at 3 mm s^{-1} may originate from a small amount of reduced mNT [3]. To satisfyingly reproduce the central part of the spectrum, a new diamagnetic species accounting for 22% of the total iron content must be introduced. The nuclear parameters were consistent with ferric ions in a tetrahedral sulfur coordination [42]. However, the isomer shift value ($\delta = 0.30$ mm s^{-1}) was at the upper limit. The dinuclear complex $[Fe_2S_2(GS)_4]^{2-}$ has been previously proposed to form in solution and nuclear parameters were published at 212 K ($\delta = 0.39$ mm s^{-1}, $\Delta E_Q = 0.68$ mm s^{-1}, [24]) and 80 K ($\delta = 0.27$ mm s^{-1}, $\Delta E_Q = 0.52$ mm s^{-1}, [40]). From these values, the formation of $[Fe_2S_2(GS)_4]^{2-}$ cannot be established for certain. The histidine coordinated iron site is undoubtedly affected by the addition of GSH. Along with nMS results, GSH binding occurs in a spatially close environment of the Fe-S cluster inducing an ejection of the latter.

4. Discussion

We explored the effect of glutathione on mNT *in vitro*. As observed previously by others [29], in the absence of oxygen the reduced form of glutathione GSH was able to partially reduce mNT cluster but this reduction decreased as the pH became lower. In the presence of oxygen, GSH induced a loss of the oxidized cluster at pH below 6.7, which became faster with decreasing pH. In our previous study the stability of the Fe-S cluster of mNT was very strongly dependent on pH between pH 6.2 and 6.7. In this study, we found a significant change in the behavior of mNT towards GSH around pH 6.5. Interestingly, one of the pKa of mNT is precisely 6.5 [43,44]. We therefore suggest that this major change in mNT behavior around pH 6.5 could be due to the protonation of a residue, eventhough no study to date has identified this protonable species. The effect of GSH was more limited on the cluster of CISD2. This oxygen-dependent cluster loss was using a radical-based mechanism and could be observed with thiol-containing molecules except cysteine that even provided a protective effect against GSH-induced cluster loss. Lastly, at pH 5.8 the spectral modifications of the UV–visible absorption and of the Mössbauer spectra were compatible with the fixation of the

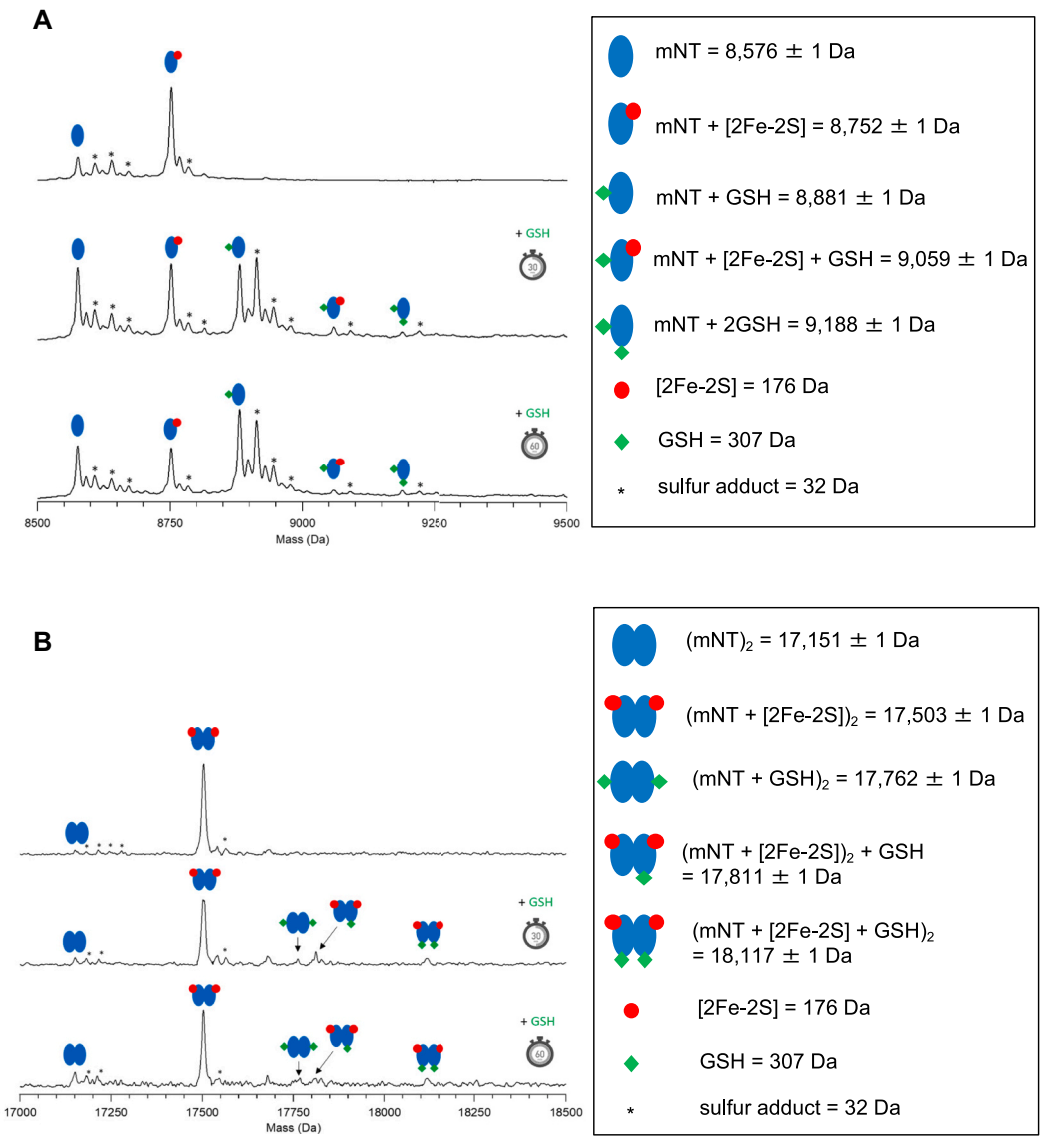

Fig. 9. GSH binds to mNT at low pH. 20 μM mNT in 50 mM ammonium acetate buffer at pH 5.8 were incubated for 30 min with 200 μM GSH under aerobic conditions and analyzed by mass spectrometry under native conditions after 30 min or 1 h. **(A)** Deconvoluted native mass spectra of monomeric species. **(B)** Deconvoluted native mass spectra of dimeric species. The spectra were annotated for the different mNT species (see insets). mNT without GSH (upper panels), mNT+ GSH (30 min) (middle panels), mNT+ GSH (60 min) (lower panels).

GSH molecule in the cluster vicinity in holo-mNT.

GSH is the most abundant intracellular low molecular mass thiol-containing molecule with concentrations in the millimolar range and a major component of the cell antioxidant defense. However, its one electron oxidation product, glutathione thiyl radical is prominent during oxidative stress or pathological conditions [45]. Glutathion thiyl radicals can mediate S-glutathionylation of proteins by conjugation of glutathione to a protein cysteine thiol that can alter protein structure, activity, subcellular localization, and interactions with molecules and partners. This redox-sensitive post-translational modification primarily protects proteins from irreversible oxidation. It also plays a key role in the regulation of a large number of cellular redox signaling platforms, particularly in mitochondria and in various physiological activities and pathological events [46–48].

E. coli SoxR is a transcription factor that governs a global defense against oxidative stress. As for NEET proteins, its [2Fe-2S] clusters act as redox switch and control its activity in response to stresses [3,7,11]. *In vitro* studies showed that GSH and other monothiol molecules disrupt its clusters using a free-radical-dependent mechanism even if the precise mechanism has yet to be demonstrated. These authors suggested that GSH could also play an inactivating role *in vivo*. The GSH-dependent disassembly of SoxR cluster is blocked by addition of sub-stoichiometric concentrations of cysteine, which could quench reactive intermediate of the cluster disruption [49] consistent with our observations with mNT. SoxR and mNT, both function as redox switches in response to stresses, react in a very similar way to thiol-containing molecules such as GSH. It has to be noticed that these two proteins have distinct coordination of their Fe-S cluster namely 4-Cys for SoxR and 3-Cys and 1-His for mNT. Based on our results and on SoxR regulation [50] we propose that GSH might be a major regulatory element of mNT activities in the cellular stress response. GSH-induced loss of the Fe-S cluster of mNT clearly involves radical species. However, similar to the SoxR situation [50], we are currently unable to identify the exact nature of the radical intermediates. As observed previously with SoxR; we have observed that the addition of cysteine at high concentration after addition of GSH blocked the GSH-induced loss of mNT Fe-S cluster (this study). We believe that cysteine may scavenge the radicals involved in the GSH-induced loss of the Fe-S cluster.

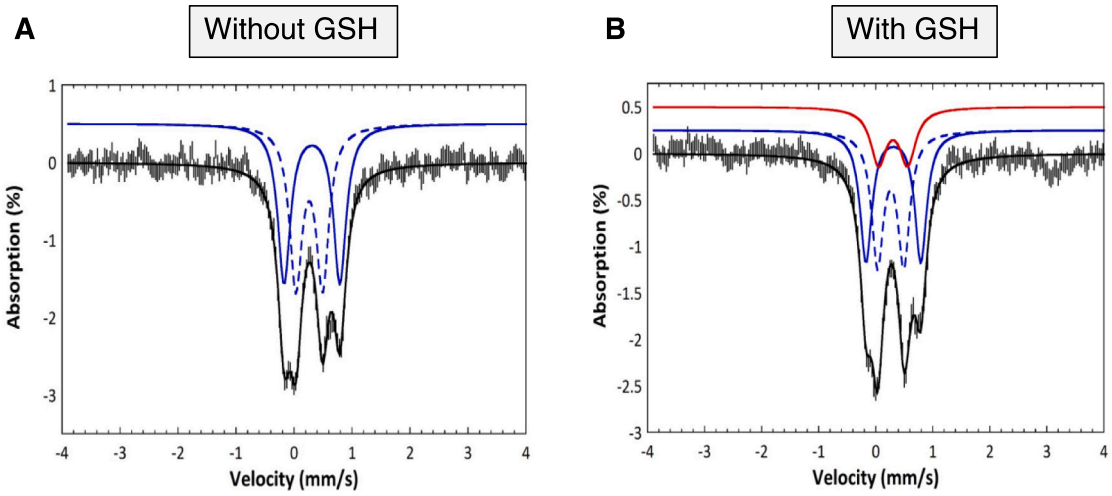

	δ (mm/s)	ΔE_Q (mm/s)	Γ (mm/s)	%
[2Fe-2S]$^{2+}$	0.26	0.46	0.26	100%
	0.31	0.96	0.26	

	δ (mm/s)	ΔE_Q (mm/s)	Γ (mm/s)	%
[2Fe-2S]$^{2+}$	0.26	0.46	0.26	78%
	0.31	0.96	0.26	
[2Fe-2S]$^{2+}$	0.30	0.51	0.34	22%
degradation				few

Fig. 10. GSH binding modifies the mNT cluster environment. Mössbauer spectra were recorded at 4.8 K with a 60 mT magnetic field applied parallel to the γ-ray with 1 mM of ^{57}Fe mNT$_{33-108}$ in 100 mM Bis-Tris pH 5.6100 mM NaCl in the absence **(A)** or the presence of 20 mM GSH **(B)**. The experimental spectrum corresponds to the black hatched lines, the simulation to the smooth black line. **(A)** The deconvolutions of the spectrum are represented by blue lines. **(B)** The spectrum was recorded after 2 h of incubation with GSH at 15 °C under aerobic conditions. The overlaid solid black lines represent the best simulations. The contributions are displayed above with the two ferric sites of mNT in a 1:1 ratio as blue solid and blue dotted lines, and the new ferric site for spectrum B as red solid line, respectively. Nuclear parameters and relative contributions are listed in the two tables with uncertainties of ±0.01 for the isomer shift δ, ±0.03 for the quadrupole splitting ΔE_Q and ± 3% for the contribution. (For interpretation of the references to colour in this figure legend, the reader is referred to the web version of this article.)

Finally, we found that one molecule of GSH could bind mNT in the vicinity of its Fe-S cluster at low pH. Single-molecule force spectroscopy analysis revealed that the Fe to His87 bond in mNT is the weakest point of the cluster coordination and can be broken without affecting the integrity of the cluster [51]. Here, despite no hard data demonstrating a direct binding of the cluster by the molecule of GSH, we propose that GSH may compete with His87 for the binding of mNT cluster at low pH. Our results do not allow us to distinguish whether GSH may bind both monomers equally or one monomer preferentially.

In the present study, CISD2 appeared to be less reactive towards GSH compared to mNT. This is consistent with our previous study, which showed that mNT and CISD2 have distinct biochemical behaviors despite their very high similarities in protein sequence and structure. Glutathione may be a major regulator of the human redox switch protein mNT as previously shown for SoxR, a bacterial redox switch protein. However, this property seems to be more specific to mNT rather than a common trait to all human NEET.

CRediT authorship contribution statement

Cécile Mons: Formal analysis, Investigation, Visualization, Writing – original draft, Writing – review & editing. **Myriam Salameh:** Investigation, Writing – original draft, Writing – review & editing. **Thomas Botzanowski:** Formal analysis, Writing – review & editing. **Martin Clémancey:** Formal analysis, Investigation. **Pierre Dorlet:** Conceptualization, Data curation, Formal analysis, Funding acquisition, Investigation, Methodology, Validation, Writing – original draft, Writing – review & editing. **Cindy Vallières:** Validation, Visualization, Writing – review & editing. **Stéphane Erb:** Visualization, Writing – review & editing. **Laurence Vernis:** Funding acquisition, Validation, Writing – review & editing. **Olivier Guittet:** Funding acquisition, Validation, Writing – review & editing. **Michel Lepoivre:** Funding acquisition, Validation, Writing – review & editing. **Meng-Er Huang:** Funding acquisition, Validation, Writing – review & editing. **Sarah Cianferani:** Conceptualization, Data curation, Funding acquisition, Methodology, Supervision, Validation, Writing – original draft, Writing – review & editing. **Jean-Marc Latour:** Conceptualization, Formal analysis, Funding acquisition, Methodology, Supervision, Writing – review & editing. **Geneviève Blondin:** Data curation, Funding acquisition, Methodology, Validation, Visualization, Writing – original draft, Writing – review & editing. **Marie-Pierre Golinelli-Cohen:** Conceptualization, Data curation, Formal analysis, Funding acquisition, Investigation, Methodology, Project administration, Supervision, Validation, Visualization, Writing – original draft, Writing – review & editing.

Declaration of competing interest

The authors declare the following financial interests/personal relationships which may be considered as potential competing interests: Mons and Salameh report financial support was provided by French Ministry of National Education. Golinelli, Blondin and Cianferani reports financial support was provided by French National Research Agency. Vernis reports financial support was provided by INSERM. Cianferani reports financial support was provided by French Proteomic Infrastructure. Botzanowski reports financial support was provided by Institut de Recherches Internationales Servier. Blondin reports financial support was provided by Labex Arcane. If there are other authors, they declare that they have no known competing financial interests or personal relationships that could have appeared to influence the work reported in this paper.

Data availability

Data will be made available on request.

Acknowledgments

We acknowledge financial support from the « Agence Nationale de la Recherche » (ANR-21-44CE-0016). The authors also warmly acknowledge the networking support from the EU COST Action FeS-BioNet (CA15133). Cécile Mons and Myriam Salameh are beneficiaries of a doctoral grant from the French Ministry of National Education, Research and Technology. Laurence Vernis is supported by the Institut National de la Santé Et de la Recherche Médicale (INSERM). This work was supported by the CNRS, the University of Strasbourg, the "Agence Nationale de la Recherche" through funding of the French Proteomic Infrastructure (ProFI; ANR-10-INBS-08-03) and of the French Infrastructure for Integrated Structural Biology (FRISBI; ANR-10-INBS-0005). Thomas Botzanowski acknowledges the Institut de Recherches Internationales Servier for funding of his PhD fellowship. Martin Clémancey and Geneviève Blondin thank the Labex Arcane and CBH-EUR-GS (ANR-17-EURE-0003) for financial support.

Appendix A. Supplementary data

Supplementary data to this article can be found online at https://doi.org/10.1016/j.jinorgbio.2024.112535.

References

[1] R. Nechushtai, A.R. Conlan, Y. Harir, L. Song, O. Yogev, Y. Eisenberg-Domovich, O. Livnah, D. Michaeli, R. Rosen, V. Ma, Y. Luo, J.A. Zuris, M.L. Paddock, Z. I. Cabantchik, P.A. Jennings, R. Mittler, Characterization of Arabidopsis NEET reveals an ancient role for NEET proteins in iron metabolism, Plant Cell 24 (2012) 2139–2154, https://doi.org/10.1105/tpc.112.097634.

[2] C.M. Kusminski, W.L. Holland, K. Sun, J. Park, S.B. Spurgin, Y. Lin, G.R. Askew, J. A. Simcox, D.A. McClain, C. Li, P.E. Scherer, MitoNEET-driven alterations in adipocyte mitochondrial activity reveal a crucial adaptive process that preserves insulin sensitivity in obesity, Nat. Med. 18 (2012) 1539–1549, https://doi.org/10.1038/nm.2899 nm.2899 [pii].

[3] I. Ferecatu, S. Gonçalves, M.-P. Golinelli-Cohen, M. Clémancey, A. Martelli, S. Riquier, E. Guittet, J.-M. Latour, H. Puccio, J.-C. Drapier, E. Lescop, C. Bouton, The diabetes drug target MitoNEET governs a novel trafficking pathway to rebuild an Fe-S cluster into cytosolic Aconitase/Iron regulatory protein 1, J. Biol. Chem. 289 (2014) 28070–28086, https://doi.org/10.1074/jbc.M114.548438.

[4] J.M. Moreno-Navarrete, M. Moreno, F. Ortega, M. Sabater, G. Xifra, W. Ricart, J. M. Fernandez-Real, CISD1 in association with obesity-associated dysfunctional adipogenesis in human visceral adipose tissue, Obesity (Silver Spring) 24 (2016) 139–147, https://doi.org/10.1002/oby.21334.

[5] Y.S. Sohn, S. Tamir, L. Song, D. Michaeli, I. Matouk, A.R. Conlan, Y. Harir, S. H. Holt, V. Shulaev, M.L. Paddock, A. Hochberg, I.Z. Cabanchick, J.N. Onuchic, P. A. Jennings, R. Nechushtai, R. Mittler, NAF-1 and mitoNEET are central to human breast cancer proliferation by maintaining mitochondrial homeostasis and promoting tumor growth, Proc. Natl. Acad. Sci. USA 110 (2013) 14676–14681, https://doi.org/10.1073/pnas.1313198110.

[6] C. Mons, T. Botzanowski, A. Nikolaev, P. Hellwig, S. Cianferani, E. Lescop, C. Bouton, M.P. Golinelli-Cohen, The H2O2-resistant Fe-S redox switch MitoNEET acts as a pH sensor to repair stress-damaged Fe-S protein, Biochemistry 57 (2018) 5616–5628, https://doi.org/10.1021/acs.biochem.8b00777.

[7] M.-P. Golinelli-Cohen, E. Lescop, C. Mons, S. Goncalves, M. Clemancey, J. Santolini, E. Guittet, G. Blondin, J.-M. Latour, C. Bouton, Redox control of the human Iron-sulfur repair protein MitoNEET activity via its Iron-sulfur cluster, J. Biol. Chem. 291 (2016) 7583–7593, https://doi.org/10.1074/jbc.M115.711218.

[8] J.A. Zuris, Y. Harir, A.R. Conlan, M. Shvartsman, D. Michaeli, S. Tamir, M. L. Paddock, J.N. Onuchic, R. Mittler, Z.I. Cabantchik, P.A. Jennings, R. Nechushtai, Facile transfer of [2Fe-2S] clusters from the diabetes drug target mitoNEET to an apo-acceptor protein, Proc. Natl. Acad. Sci. USA 108 (2011) 13047–13052, https://doi.org/10.1073/pnas.1109986108.

[9] C.H. Lipper, M.L. Paddock, J.N. Onuchic, R. Mittler, R. Nechushtai, P.A. Jennings, Cancer-related NEET proteins transfer 2Fe-2S clusters to Anamorsin, a protein required for cytosolic Iron-sulfur cluster biogenesis, PLoS One 10 (2016) e0139699, https://doi.org/10.1371/journal.pone.0139699.

[10] M.-P. Golinelli-Cohen, C. Bouton, Fe-S proteins acting as redox switch: new key actors of cellular adaptive responses, Curr. Chem. Biol. 11 (2017) 70–88, https://doi.org/10.2174/2212796811666170406163809.

[11] R. Nechushtai, O. Karmi, K. Zuo, H.-B. Marjault, M. Darash-Yahana, Y.-S. Sohn, S. D. King, S.I. Zandalinas, P. Carloni, R. Mittler, The balancing act of NEET proteins: Iron, ROS, calcium and metabolism, Biochimica et Biophysica Acta (BBA) - Molecular Cell Research 1867 (2020) 118805, https://doi.org/10.1016/j.bbamcr.2020.118805.

[12] M. Salameh, S. Riquier, O. Guittet, M.-E. Huang, L. Vernis, M. Lepoivre, M.-P. Golinelli-Cohen, New insights of the NEET protein CISD2 reveals distinct features compared to its close mitochondrial homolog mitoNEET, Biomedicines 9 (2021) 384, https://doi.org/10.3390/biomedicines9040384.

[13] E.V. Kalinina, N.N. Chernov, M.D. Novichkova, Role of glutathione, glutathione transferase, and glutaredoxin in regulation of redox-dependent processes, Biochem. Mosc. 79 (2015) 1562–1583, https://doi.org/10.1134/s0006297914130082.

[14] M. Deponte, The incomplete glutathione puzzle: just guessing at numbers and figures? Antioxid. Redox Signal. 27 (2017) 1130–1161, https://doi.org/10.1089/ars.2017.7123.

[15] D. Matuz-Mares, H. Riveros-Rosas, M.M. Vilchis-Landeros, H. Vazquez-Meza, Glutathione participation in the prevention of cardiovascular diseases, Antioxidants (Basel) 10 (2021), https://doi.org/10.3390/antiox10081220.

[16] C.A. Labarrere, G.S. Kassab, Glutathione: a Samsonian life-sustaining small molecule that protects against oxidative stress, ageing and damaging inflammation, Front. Nutr. 9 (2022), https://doi.org/10.3389/fnut.2022.1007816.

[17] E. Szliszka, Z.P. Czuba, M. Domino, B. Mazur, G. Zydowicz, W. Krol, Ethanolic extract of propolis (EEP) enhances the apoptosis- inducing potential of TRAIL in cancer cells, Molecules 14 (2009) 738–754, https://doi.org/10.3390/molecules.

[18] K. Sipos, H. Lange, Z. Fekete, P. Ullmann, R. Lill, G. Kispal, Maturation of cytosolic iron-sulfur proteins requires glutathione, J. Biol. Chem. 277 (2002) 26944–26949, https://doi.org/10.1074/jbc.M200677200.

[19] C. Kumar, A. Igbaria, B. D'Autreaux, A.G. Planson, C. Junot, E. Godat, A. K. Bachhawat, A. Delaunay-Moisan, M.B. Toledano, Glutathione revisited: a vital function in iron metabolism and ancillary role in thiol-redox control, EMBO J. 30 (2011) 2044–2056, https://doi.org/10.1038/emboj.2011.105.

[20] R.C. Hider, X. Kong, Iron speciation in the cytosol: an overview, Dalton Trans. 42 (2013) 3220–3229, https://doi.org/10.1039/c2dt32149a.

[21] C. Johansson, A.K. Roos, S.J. Montano, R. Sengupta, P. Filippakopoulos, K. Guo, F. von Delft, A. Holmgren, U. Oppermann, K.L. Kavanagh, The crystal structure of human GLRX5: iron-sulfur cluster co-ordination, tetrameric assembly and monomer activity, Biochem. J. 433 (2011) 303–311, https://doi.org/10.1042/BJ20101286.

[22] V. Srinivasan, A.J. Pierik, R. Lill, Crystal structures of nucleotide-free and glutathione-bound mitochondrial ABC transporter Atm1, Science 343 (2014) 1137–1140, https://doi.org/10.1126/science.1246729.

[23] S.A. Pearson, C. Wachnowsky, J.A. Cowan, Defining the mechanism of the mitochondrial Atm1p [2Fe-2S] cluster exporter, Metallomics 12 (2020) 902–915, https://doi.org/10.1039/c9mt00286c.

[24] W. Qi, J. Li, C.Y. Chain, G.A. Pasquevich, A.F. Pasquevich, J.A. Cowan, Glutathione complexed Fe-S centers, J. Am. Chem. Soc. 134 (2012) 10745–10748, https://doi.org/10.1021/ja302186j.

[25] C. Wachnowsky, I. Fidai, J.A. Cowan, Iron–sulfur cluster biosynthesis and trafficking – impact on human disease conditions, Metallomics 10 (2018) 9–29, https://doi.org/10.1039/c7mt00180k.

[26] S. Sen, J.A. Cowan, Role of protein-glutathione contacts in defining glutaredoxin-3 [2Fe-2S] cluster chirality, ligand exchange and transfer chemistry, J. Biol. Inorg. Chem. 22 (2017) 1075–1087, https://doi.org/10.1007/s00775-017-1485-9.

[27] M.S. Alam, S.K. Garg, P. Agrawal, Studies on structural and functional divergence among seven WhiB proteins of mycobacterium tuberculosis H37Rv, FEBS J. 276 (2009) 76–93, https://doi.org/10.1111/j.1742-4658.2008.06755.x.

[28] H. Ding, B. Demple, Thiol-mediated disassembly and reassembly of [2Fe-2S] clusters in the redox-regulated transcription factor SoxR, Biochemistry 37 (1998) 17280–17286, https://doi.org/10.1021/bi980532g.

[29] A.P. Landry, H. Ding, Redox control of human mitochondrial outer membrane protein MitoNEET [2Fe-2S] clusters by biological thiols and hydrogen peroxide, J. Biol. Chem. 289 (2014) 4307–4315, https://doi.org/10.1074/jbc.M113.542050.

[30] F.J. Romero, I. Ordoñez, A. Arduini, E. Cadenas, The reactivity of thiols and disulfides with different redox states of myoglobin, Redox and addition reactions and formation of thiyl radical intermediates, J. Biol. Chem. 267 (1992) 1680–1688.

[31] M.E. Anderson, Determination of Glutathione and Glutathione Disulfide in Biological Samples, 2024.

[32] C. Mons, I. Ferecatu, S. Riquier, E. Lescop, C. Bouton, M.-P. Golinelli-Cohen, Combined biochemical, biophysical and cellular methods to study Fe-S cluster transfer and cytosolic aconitase repair by mitoNEET, Methods Enzymol. 595 (2017) 83–106, https://doi.org/10.1016/bs.mie.2017.07.010.

[33] G. Candiano, M. Bruschi, L. Musante, L. Santucci, G.M. Ghiggeri, B. Carnemolla, P. Orecchia, L. Zardi, P.G. Righetti, Blue silver: a very sensitive colloidal Coomassie G-250 staining for proteome analysis, Electrophoresis 25 (2004) 1327–1333, https://doi.org/10.1002/elps.200305844.

[34] M.M. Dicus, A. Conlan, R. Nechushtai, P.A. Jennings, M.L. Paddock, R.D. Britt, S. Stoll, Binding of histidine in the (Cys)3(his)1-coordinated [2Fe-2S] cluster of human mitoNEET, J. Am. Chem. Soc. 132 (2010) 2037–2049, https://doi.org/10.1021/ja909359g.

[35] D. Hofstetter, T. Nauser, W.H. Koppenol, Hydrogen exchange equilibria in glutathione radicals: rate constants, Chem. Res. Toxicol. 23 (2010) 1596–1600, https://doi.org/10.1021/tx100185k.

[36] C.C. Winterbourn, D. Metodiewa, Reaction of superoxide with glutathione and other thiols, Methods Enzymol. 251 (1995) 81–86, https://doi.org/10.1016/0076-6879(95)51112-1.

[37] Y. Sugiura, H. Tanaka, Iron-sulfide chelates of some sulfur-containing peptides as model complex of non-heme iron proteins, Biochem. Biophys. Res. Commun. 46 (1972) 335–340, https://doi.org/10.1016/s0006-291x(72)80143-8.

[38] I. Fidai, C. Wachnowsky, J.A. Cowan, Glutathione-complexed [2Fe-2S] clusters function in Fe-S cluster storage and trafficking, J. Biol. Inorg. Chem. 21 (2016) 887–901, https://doi.org/10.1007/s00775-016-1387-2.

[39] M. Invernici, G. Selvolini, J.M. Silva, G. Marrazza, S. Ciofi-Baffoni, M. Piccioli, Interconversion between [2Fe-2S] and [4Fe-4S] cluster glutathione complexes,

Chem. Commun. (Camb.) 58 (2022) 3533–3536, https://doi.org/10.1039/d1cc03566e.
[40] C. Bonfio, L. Valer, S. Scintilla, S. Shah, D.J. Evans, L. Jin, J.W. Szostak, D. D. Sasselov, J.D. Sutherland, S.S. Mansy, UV-light-driven prebiotic synthesis of iron–sulfur clusters, Nat. Chem. 9 (2017) 1229–1234, https://doi.org/10.1038/nchem.2817.
[41] A.R. Conlan, M.L. Paddock, C. Homer, H.L. Axelrod, A.E. Cohen, E.C. Abresch, J. A. Zuris, R. Nechushtai, P.A. Jennings, Mutation of the his ligand in mitoNEET stabilizes the 2Fe-2S cluster despite conformational heterogeneity in the ligand environment, Acta Crystallogr. D Biol. Crystallogr. 67 (2011) 516–523, https://doi.org/10.1107/S0907444911011577.
[42] K. Stegmaier, C.M. Blinn, D.F. Bechtel, C. Greth, H. Auerbach, C.S. Müller, V. Jakob, E.J. Reijerse, D.J.A. Netz, V. Schünemann, A.J. Pierik, Apd1 and Aim32 are prototypes of Bishistidinyl-coordinated non-Rieske [2Fe–2S] proteins, J. Am. Chem. Soc. 141 (2019) 5753–5765, https://doi.org/10.1021/jacs.8b13274.
[43] D.W. Bak, J.A. Zuris, M.L. Paddock, P.A. Jennings, S.J. Elliott, Redox characterization of the FeS protein MitoNEET and impact of thiazolidinedione drug binding, Biochemistry 48 (2009) 10193–10195, https://doi.org/10.1021/bi9016445.
[44] D.W. Bak, S.J. Elliott, Conserved hydrogen bonding networks of MitoNEET tune Fe-S cluster binding and structural stability, Biochemistry 52 (2013) 4687–4696, https://doi.org/10.1021/bi400540m.
[45] C. Schoneich, Thiyl radicals and induction of protein degradation, Free Radic. Res. 50 (2016) 143–149, https://doi.org/10.3109/10715762.2015.1077385.
[46] R.J. Mailloux, C. Grayson, O. Koufos, Regulation of mitochondrial hydrogen peroxide availability by protein S-glutathionylation, Cells 12 (2022), https://doi.org/10.3390/cells12010107.
[47] S. Vrettou, B. Wirth, S-Glutathionylation and S-Nitrosylation in mitochondria: focus on homeostasis and neurodegenerative diseases, Int. J. Mol. Sci. 23 (2022), https://doi.org/10.3390/ijms232415849.
[48] P.T. Kang, C.-L. Zhang, L Fau - Chen, J. Chen Cl Fau - Chen, K.B. Chen, J Fau - Green, Y.-R. Green Kb Fau - Chen, and Y.R. Chen, Protein thiyl radical mediates S-glutathionylation of complex I, Free Radic. Biol. Med. 53 (2012) 962–973, https://doi.org/10.1016/j.freeradbiomed.2012.05.025.
[49] H. Ding, E. Hidalgo, B. Demple, The redox state of the [2Fe-2S] clusters in SoxR protein regulates its activity as a transcription factor, J. Biol. Chem. 271 (1996) 33173–33175, https://doi.org/10.1074/jbc.271.52.33173.
[50] Q. Wang, X. Lu, H. Yang, H. Yan, Y. Wen, Redox-sensitive transcriptional regulator SoxR directly controls antibiotic production, development and thiol-oxidative stress response in Streptomyces avermitilis, microb, Biotechnol 15 (2022) 561–576, https://doi.org/10.1111/1751-7915.13813.
[51] G. Song, X. Ding, H. Liu, G. Yuan, F. Tian, S. Shi, Y. Yang, G. Li, P. Zheng, Single-molecule force spectroscopy reveals that the Fe-N bond enables multiple rupture pathways of the 2Fe2S cluster in a MitoNEET monomer, Anal. Chem. 92 (2020) 14783–14789, https://doi.org/10.1021/acs.analchem.0c03536.